



GLOBAL JOURNAL OF SCIENCE FRONTIER RESEARCH: A
PHYSICS AND SPACE SCIENCE

Volume 17 Issue 1 Version 1.0 Year 2017

Type : Double Blind Peer Reviewed International Research Journal

Publisher: Global Journals Inc. (USA)

Online ISSN: 2249-4626 & Print ISSN: 0975-5896

Simulating the Second Moment of NMR Spectral Line in Ammonium Chloride Single Crystal

By F. I. Bashirov & N. K. Gaisin

Kazan Federal University

Abstract- Innovative technique of simulating the second moment of NMR spectral line broadened owing to the magnetic dipole-dipole interaction in crystals with internal molecular motion is suggested. The local hindered molecular motion (HMM) is approximated by the extended angular jump model. The resulting expression of the second moment allows one to evaluate the crystal structure distortion and the dynamical parameters of HMM. The presented theory agrees with the experimental anisotropic second moment of proton NMR spectral line in whole temperature region of the ammonium chloride single crystal investigation.

Keywords: *crystallographic point symmetry; hindered molecular motion; nuclear magnetic resonance; second moment; single crystal; symmetry distortion.*

GJSFR-A Classification: FOR Code: 020399



Strictly as per the compliance and regulations of :



Simulating the Second Moment of NMR Spectral Line in Ammonium Chloride Single Crystal

F. I. Bashirov ^α & N. K. Gaisin ^ο

Abstract- Innovative technique of simulating the second moment of NMR spectral line broadened owing to the magnetic dipole-dipole interaction in crystals with internal molecular motion is suggested. The local hindered molecular motion (HMM) is approximated by the extended angular jump model. The resulting expression of the second moment allows one to evaluate the crystal structure distortion and the dynamical parameters of HMM. The presented theory agrees with the experimental anisotropic second moment of proton NMR spectral line in whole temperature region of the ammonium chloride single crystal investigation.

Keywords: crystallographic point symmetry; hindered molecular motion; nuclear magnetic resonance; second moment; single crystal; symmetry distortion.

I. INTRODUCTION

The use of spectroscopy techniques such as neutron, Raman, infrared, dielectric, electron, nuclear magnetic and electric quadrupole resonance spectroscopy to study condensed state physics problems has several advantages. This includes the detailed nature of the information, which can be obtained on structural and dynamical properties, and the definiteness of the interpretation, which can be given to the data. The theoretical studying of hindered molecular motion (HMM) dynamics is normally carried out by examining the time depended auto-correlation function (ACF) of a physical quantity of the molecule. A notable progress has been made in the theory of HMM by using the properties of continuous [1] and point [2, 3] symmetry groups.

The second moment of NMR spectral line broadened owing to the magnetic dipole-dipole interaction of nuclear spins is serving as one of main probes of HMM in crystalline substances [4-7]. Measuring the second moment allows one to testing various models of HMM taking place in condensed matter.

The basic statements of the well-known HMM models have been carefully discussed in [2, 8]. The

most recent developed model, the so-called extended angular jump model (EAJM), is well appropriate to exploring HMM of symmetrical molecules in single crystals, powders, and liquids. It was successfully applied to examine the rates of nuclear magnetic relaxation [9-11], the relative intensities of Raman light scattering [11, 13], dielectric [14, 15] and infrared [13] absorption, and the incoherent neutron scattering function [7, 8, and 16] in mono- and polycrystalline molecular media.

Recently, EAJM-approach was used by describing the intramolecular contribution to the second moment of NMR line shape [17]. This time, we decided to expand this application up to ability of simulating whole NMR spectral line second moment in molecular crystals without any restriction on the temperature region. So, this paper is devoted to add EAJM-approach to simulating the second moment of NMR absorption line broadened owing to the magnetic dipole-dipole interaction of homo- and hetero-nuclear spins in perfect and symmetry distorted crystals. We shall consider the contributions of both intra- and inter-molecular dipole-dipole interactions to the 2nd moment. The validity of the application will be verified by approximating the known experimental data on the 2nd moment of the proton NMR spectral line measured for two main directions of the external magnetic field in the single crystal of ammonium chloride at large temperature region [18].

II. BASICS OF THE THEORY OF NMR 2ND MOMENT M_2 IN MOLECULAR CRYSTALS

The second moment of NMR spectral line M_2 broadened owing to magnetic dipole-dipole interaction of identical resonant nuclear spins in molecular crystals can be simulated by using the following basic expression [3-6]:

$$M_2 = \frac{1}{N_i} \sum_{i=1}^{N_i} \sum_{j \neq i} \frac{3}{4} \hbar^2 \gamma_j^2 r_{ji}^{-6} I_j (I_j + 1) (3 \cos^2 \theta_{ji} - 1)^2, \quad (1)$$

where the subscript i labels the resonant nuclear spins of a molecule and the symbol N_i designates the number of such spins, the subscript j labels all resonant nuclear spins of the crystal; the symbols γ and I denote respectively

Author α: Corresponding author, Department of General Physics, Kazan Federal University, 420111, Kazan, Russian Federation.

e-mail: fbashir@mail.ru

Author ο: Department of Physics, Kazan Technological University, 420015, Kazan, Russian Federation.

the gyromagnetic ratio and the quantum number of the nuclei; $\hbar = 1.0544 \cdot 10^{-34}$ J-s is Planck's constant, θ_{ji} is the polar angle that forms the internuclear vector $\mathbf{r}_{ji} = r_{ji} (r_{ji}, \varphi_{ji}, \theta_{ji})$ with respect to the intensity vector of stationary magnetic field \mathbf{B}_0 allocating the laboratory reference frame (LRF). The azimuthal angle φ_{ji} can be any.

In the case of the direction of intramolecular vector $\mathbf{r}_{ji} (r_{ji}, \varphi_{ji}, \theta_{ji})$ changes accidentally, its spherical angles ($\varphi_{ji}, \theta_{ji}$) as well as some intermolecular vectors present random functions of time. As a result, spectral distribution of NMR signal is modified. However, the intramolecular and intermolecular vectors effect on NMR signal by different way. Consequently, simulating the NMR second moment M_2 is to be performed by accounting for two additive contributions – intramolecular $M_2^{(intra)}$ and intermolecular $M_2^{(inter)}$:

$$M_2 = M_2^{(intra)} + M_2^{(inter)}. \quad (2)$$

a) *Intramolecular contribution – $M_2^{(intra)}$*

The intramolecular contribution $M_2^{(intra)}$ to the total second moment M_2 accounting for the hindered motion of intramolecular vectors can be presented in the form [19]:

$$M_2^{(intra)} = \frac{1}{N_i} \sum_{i=1}^{N_i} \sum_{j \neq i} \left[\frac{3}{4} \hbar^2 \gamma_j^2 I_j (I_j + 1) \cdot \int_{-\delta v_i}^{\delta v_i} J_{ji}^{(0)}(\omega_i) dv_i \right], \quad (3)$$

where

$$J_{ji}^{(0)}(\omega_i) = \int_{-\infty}^{+\infty} K_{ji}^{(0)}(t) \exp(i\omega_i t) dt \quad (4)$$

is the no normalized spectral density function (SDF) of the autocorrelation function

$$K_{ji}^{(0)}(t) = \langle F_{ji}^{(0)}(t) F_{ji}^{(0)*}(t + \tau) \rangle \quad (5)$$

of the lattice part of spin-spin interaction Hamiltonian

$$F_{ji}^{(0)}(t) = r_{ji}^{-3} (3 \cos^2 \theta_{ji}(t) - 1) = \left(\frac{16\pi}{5} \right)^{1/2} r_{ji}^{-3} Y_0^{(2)}[\varphi_{ji}, \theta_{ji}(t)]. \quad (6)$$

The quantity $Y_0^{(2)}[\varphi_{ji}, \theta_{ji}(t)]$ is the zero component of the 2nd rank normalized spherical function. In Equation (3), the integration has to be performed within the limits of the double line width from $-\delta v_i$ up to $+\delta v_i$, where $v_i = \omega_i / 2\pi = \gamma_i B_0$ is the resonance frequency of i -th spins, B_0 – the module of induction vector of the static magnetic field, γ_i – the gyromagnetic ratio of resonant nuclei, $\delta v_i = 1/T_{2i}$ (T_{2i} is the spin-spin relaxation time).

The outcomes of simulating Equation (3) depend on the physical model of molecular motion. With respect to the goal of the present studying, EAJM-approach will be used as the model of HMM [2, 8]. Within the framework of that model, the analytical expression of normalized SDF $J_0^{(2)}(\omega_i)$ of the tensor component $Y_0^{(2)}[\phi(t), \vartheta(t)]$ is presented for a single crystal sample by

$$J_0^{(2)}(\omega) = J_0^{(2)}(q_\alpha, \phi, \vartheta, \omega) = \frac{5}{2\pi} \sum_{\alpha} \sum_{l=0}^2 \frac{q_\alpha \tau_\alpha}{1 + (\omega \tau_\alpha)^2} a_{\alpha l 0}(\phi) \cos^{2l} \vartheta. \quad (7)$$

It is noted that the angles φ_{ji} and θ_{ji} of the internuclear vector \mathbf{r}_{ji} do not present explicitly in Equation (7). Instead, there are two spherical angles ϕ and ϑ , by which orientation of the crystallographic reference frame sets up in the axial laboratory one. The subscript α labels irreducible representations (IR) Γ_α of the HMM point symmetry group G.

By accounting for Equation (7), the no normalized SDF $J_{ji}^{(0)}(\omega_i)$ takes the form:

$$J_{ji}^{(0)}(\omega_i) = J_{ji}^{(0)}(q_\alpha, \phi, \vartheta, \omega_i) = \frac{16\pi}{5} r_{ji}^{-6} J_0^{(2)}(q_\alpha, \phi, \vartheta, \omega_i) =$$

$$8 r_{ji}^{-6} \sum_{\alpha} \sum_{l=0}^2 \frac{q_{\alpha} \tau_{\alpha}}{1 + (\omega_i \tau_{\alpha})^2} a_{\alpha l 0}(\phi) \cos^{2l} \vartheta. \quad (8)$$

The rated expressions of the factors $a_{\alpha l 0}(\phi)$ are tabulated explicitly as functions of azimuthal angle ϕ for all crystallographic point symmetry groups of pure rotation in [2,8]. A quantity q_{α} , the dynamic weight of IR Γ_{α} of the group G, is playing a role of adjustable parameter of the theory that has to be experimentally determined. It satisfies the normalization condition: $\sum q_{\alpha} = 1$. For ideal symmetry of HMM, a dynamic weight q_{α} reduces its static value value equals to the dimension of IR Γ_{α} of the group G. The parameter τ_{α} , the HMM correlation time adapted to Γ_{α} , relates the expression:

$$\tau_{\alpha} = (1 - \chi_{\alpha E}^{-1} \sum_i p_i \chi_{\alpha i})^{-1} \tau, \quad (9)$$

where $\chi_{\alpha i}$ and $\chi_{\alpha E}$ are the characters of i -th and identical classes, respectively, p_i – the probability of the fundamental act of motion appropriate to i -th class of the group G, and τ – a mean time between two successive steps of motion. The time τ is ordered to Arrhenius low:

$$\tau = \tau_0 \exp(E_a/RT), \quad (10)$$

where E_a is the height of activation energy barrier averaged on the HMM symmetry group, τ_0 is a mean time between two sequential attempts to overlap the barrier.

By substituting Equation (8) in Equation (3), we shall obtain the 2nd moment expression specified by the intramolecular action of resonant spins j to target resonant spins i in analytical form by

$$M_2^{(\text{intra})} = \frac{6}{N_i} \sum_{i=1}^{N_i} \sum_{j \neq i} \hbar^2 \gamma_j^2 r_{ji}^{-6} I_j(I_j + 1) \int_{-\delta v_i}^{\delta v_i} \left[\sum_{\alpha} \sum_{l=0}^2 \frac{q_{\alpha} \tau_{\alpha}}{1 + (2\pi v_i \tau_{\alpha})^2} a_{\alpha l 0}(\phi) \cos^{2l} \vartheta \right] dv_i. \quad (11)$$

By performing the prescribed integration, we are obtaining:

$$M_2^{(\text{intra})} = \frac{6}{\pi N_i} \sum_{i=1}^{N_i} \sum_{j \neq i} \hbar^2 \gamma_j^2 r_{ji}^{-6} I_j(I_j + 1) \sum_{\alpha} \sum_{l=0}^2 q_{\alpha} a_{\alpha l 0}(\phi) \cos^{2l} \vartheta \arctg(2\pi \cdot \delta v_i \cdot \tau_{\alpha}). \quad (12)$$

For a powder, by averaging over the angles ϕ and ϑ , Equation (12) reduces to:

$$M_2^{(\text{intra|pow})} = \frac{6}{5\pi N_i} \sum_{i=1}^{N_i} \sum_{j \neq i} \hbar^2 \gamma_j^2 r_{ji}^{-6} I_j(I_j + 1) \sum_{\alpha} q_{\alpha} \arctg(2\pi \cdot \delta v_i \cdot \tau_{\alpha}). \quad (13)$$

In a regime of a fast molecular motion, the inequality $(2\pi \cdot \delta v_i \cdot \tau_{\alpha}) \ll 1$ is valid that follows the equality $\arctg(2\pi \cdot v_i \cdot \tau_{\alpha}) = 0$. In this case the dipole-dipole contribution to the second moment vanishes, that is, $M_2^{(\text{intra})} = 0$, and so-called phenomenon of "spectral line narrowing" or "bandwidth narrowing" is observed.

Alternatively, in the case of a slow motion regime, inequality $(2\pi \cdot v_i \cdot \tau_{\alpha}) \gg 1$ followed by equality $\arctg(2\pi \cdot v_i \cdot \tau_{\alpha}) \pi/2$ is valid. Furthermore, taking into account the normalization condition $\sum_{\alpha} q_{\alpha} = 1$, Equation (13) reduces down to a permanent value:

$$M_2^{(\text{intra|pow})} = \frac{3}{5N_i} \sum_{i=1}^{N_i} \sum_{j \neq i} \hbar^2 \gamma_j^2 r_{ji}^{-6} I_j(I_j + 1) \quad (14)$$

presented earlier by Abraham and Lösche [5, 6].

For single crystals, Equation (12) reduces to an expression retaining the angular dependence of the 2nd moment produced by homonuclear dipole-dipole interaction in the slow molecular motion regime:

$$M_{2ji}^{(\text{intra})} = \frac{3}{N_i} \sum_{i=1}^{N_i} \sum_{j \neq i} \hbar^2 \gamma_j^2 r_{ji}^{-6} I_j(I_j + 1) \sum_{\alpha} \sum_{l=0}^2 q_{\alpha} a_{\alpha l 0}(\phi) \cos^{2l} \vartheta. \quad (15)$$

As to the second moment contribution produced by the heteronuclear dipole-dipole interaction, the respective formula differs from that above presented by the factor 4/9 [20]. In this case, Equation (15) has to be replaced by

$$M_{2si}^{(\text{intra})} = \frac{4}{3N_i} \sum_{i=1}^{N_i} \sum_s \hbar^2 \gamma_s^2 r_{si}^{-6} I_s(I_s + 1) \sum_{\alpha} \sum_{l=0}^2 q_{\alpha} a_{\alpha l 0}(\phi) \cos^{2l} \vartheta, \quad (16)$$

where the subscript s labels no resonant nuclear spins of the molecule and N_s is the number of such spins.

b) *Intermolecular contribution* $-M_2^{(\text{inter})}$

The expression of intermolecular contribution to the 2nd moment $M_2^{(\text{inter})}$ associated with homonuclear interaction will be derived by modifying the basic Equation (1) to a form involving the spherical harmonics. We shall replace the angular dependent multiplier $(3 \cos^2 \theta_{ji} - 1)^2$ by its equivalent doublet $\frac{16\pi}{5} |Y_0^{(2)}(\varphi_{ji}, \theta_{ji})|^2$, where $Y_0^{(2)}(\varphi_{ji}, \theta_{ji})$ is a normalized spherical harmonic (function) of the 2nd order, a unit spherical tensor of the 2nd rank. Notice: (2) $Y_0^{(2)}(\varphi_{ji}, \theta_{ji})$ has no dependence of the azimuthal angle φ_{ji} in this particular case of the zero component of unit spherical tensor of the 2nd rank. Thus, we are rewriting expression (1) in terms of spherical tensors as:

$$M_2^{(\text{inter})} = \frac{12\pi}{5N_i} \sum_{i=1}^{N_i} \sum_{j=1}^{N_j} \hbar^2 \gamma_i^2 r_{ji}^{-6} I_i(I_i + 1) |Y_0^{(2)}(\varphi_{ji}, \theta_{ji})|^2, \quad (17)$$

where N_i is the number of intramolecular resonant spins and N_j is outer (relative to the target molecule) resonant spins. The angles θ_{ji} and φ_{ji} are determined in the LRF.

Nevertheless, it is helpful to assign the internuclear vectors in the crystallographic reference frame (CRF). To produce this change, we shall transform spherical tensors from CRF to LRF by rotation to the three-dimensional Euler angles (ϕ, ϑ, ξ) according to the rule [21]:

$$Y_0^{(2)}(\varphi', \theta') = \sum_{m=-2}^2 D_{0m}^{(2)}(\phi, \vartheta, \xi) Y_m^{(2)}(\varphi, \theta), \quad (18)$$

where (2) $D_{0m}^{(2)}(\phi, \vartheta, \xi)$ is an element of Wigner matrix. Now, we can rewrite Equation (17) as:

$$M_2^{(\text{inter})} = \frac{12\pi}{5N_i} \sum_{i=1}^{N_i} \sum_{j=1}^{N_j} \hbar^2 \gamma_i^2 r_{ji}^{-6} I_i(I_i + 1) \left[\sum_{m=-2}^2 D_{0m}^{(2)}(\phi, \vartheta, \xi) Y_m^{(2)}(\varphi_{ji}, \theta_{ji}) \right]^2. \quad (19)$$

By replacing $D_{0m}^{(2)}(\phi, \vartheta, \xi) = \sqrt{(4\pi/5)} Y_m^{(2)}(\vartheta, \phi)$ and renaming $M_2^{(\text{inter})} = M_{2ji}^{(\text{inter})}(\phi, \vartheta)$ we shall transform Equation (19) to

$$M_{2ji}^{(\text{inter})}(\phi, \vartheta) = \frac{48\pi^2}{25N_i} \sum_{i=1}^{N_i} \sum_{j=1}^{N_j} \hbar^2 \gamma_i^2 r_{ji}^{-6} I_i(I_i + 1) \left[\sum_{m=-2}^2 Y_m^{(2)}(\phi, \vartheta) Y_m^{(2)}(\varphi_{ji}, \theta_{ji}) \right]^2, \quad (20)$$

where ϕ and ϑ are the spherical angles of the vector \mathbf{B}_0 assigned in LRF, and φ_{ji} and θ_{ji} are those of the internuclear vector \mathbf{r}_{ji} determined in CRF, the subscripts i and j label the resonant homonuclear spins.

By multiplying Equation (20) by the factor 4/9 and replacing subscript j by v to label no resonant nuclear spins, we shall get the heteronuclear analog of the intermolecular contribution to the 2nd moment $M_{2vi}^{(\text{inter})}$



$$M_{2vi}^{(\text{inter})}(\phi, \vartheta) = \frac{64\pi^2}{75N_i} \sum_{i=1}^{N_i} \sum_{v=1}^{N_v} \hbar^2 \gamma_v^2 r_{vi}^{-6} I_v(I_v + 1) \left[\sum_{m=-2}^2 Y_m^{(2)}(\phi, \vartheta) Y_m^{(2)}(\phi_{vi}, \theta_{vi}) \right]^2. \quad (21)$$

c) Total expression of the 2nd moment – M_2

Taking into account above presented Equations (2), (12), (15), (16), (20), and (21), we are able to write the total expression of the NMR 2nd moment $M_2^{(T)}(\phi, \vartheta)$:

$$M_2^{(T)}(\phi, \vartheta) = \frac{2\hbar^2}{N_i\pi} \sum_{i=1}^{N_i} \left[3 \sum_{\substack{j=1 \\ j \neq i}}^{N_i-1} \gamma_i^2 I_i(I_i + 1) r_{ji}^{-6} + \frac{4}{3} \sum_{s=1}^{N_s} \gamma_s^2 I_s(I_s + 1) r_{si}^{-6} \right] \cdot \\ \sum_{\alpha} \sum_{l=0}^2 q_{\alpha} \arctg(2\pi \cdot \delta v_i \cdot \tau_{\alpha}) a_{\alpha l 0}(\phi) \cos^{2l} \vartheta + \\ \frac{48\pi^2 \hbar^2}{25N_i} \sum_{i=1}^{N_i} \sum_{j'=1}^{N_{j'}} \gamma_i^2 I_i(I_i + 1) r_{j'i}^{-6} \left[\sum_{m=-2}^2 Y_m^{(2)}(\phi, \vartheta) Y_m^{(2)}(\phi_{j'i}, \theta_{j'i}) \right]^2 + \\ \frac{64\pi^2 \hbar^2}{75N_i} \sum_{i=1}^{N_i} \sum_{v=1}^{N_v} \gamma_v^2 I_v(I_v + 1) r_{vi}^{-6} \left[\sum_{m=-2}^2 Y_m^{(2)}(\phi, \vartheta) Y_m^{(2)}(\phi_{vi}, \theta_{vi}) \right]^2. \quad (22)$$

The temperature dependence of Equation (22) takes place implicitly by means of the dynamical variable τ_{α} included in intramolecular part of the 2nd moment. Besides, owing to the temperature dependence of the components r_{ji} , r_{vi} , ϕ_{ji} , θ_{ji} , ϕ_{vi} and θ_{vi} of the internuclear vectors \mathbf{r}_{ji} , \mathbf{r}_{vi} , the intermolecular part of the 2nd moment has to be also temperature depended. Meanwhile, it is reasonable to assume that small fluctuations of angles $\phi_{j'i}$, $\theta_{j'i}$ and ϕ_{vi} , θ_{vi} about their equilibrium values can't give notable change of local magnetic field on the sites of target protons. Therefore, by evaluating the 2nd moment in the fast motion regime, we shall take into account only the dependence of internuclear distances r_{ji} and r_{vi} of temperature.

It is timely to remind the meaning of some quantities and labels displayed in Equation (22):

N_i is the number of identical resonant nuclear spins of a target molecule,

i and j label intramolecular resonant nuclear spins,

j' labels resonant spins outer relative to the target molecule,

s – intramolecular no resonant heteronuclear spins,

v – no resonant heteronuclear spins outer relative to the target molecule,

ϕ and ϑ designate the spherical angles of the axial magnetic field direction with respect to CRF,

ϕ_{ji} and θ_{ji} – the spherical angles of \mathbf{r}_{ji} - internuclear vector fixed in the CRF,

q_{α} and $a_{\alpha l 0}$ – the quantities of the EAJM-approach theory [2, 8].

III. APPLICATION TO THE SINGLE CRYSTAL OF AMMONIUM CHLORIDE NH_4Cl

a) Overview

Ammonium chloride being one of the most studied substances is frequently used as a touchstone of the validity of various theories on the structure and physical properties of crystals. It is an ionic crystal, which ammonium ions exhibit random reorientation and consequently they have no permanent orientation ordering. Unit cell of NH_4Cl is a body-centered cube of CsCl type. At center of a cubic cell, a tetrahedron of ammonium cation NH_4^+ is placed, and its corners are occupied by chlorine anions Cl^- . The lattice parameter is $r_{\text{Cl-Cl}} = r_{\text{N-N}} = (3.844 \pm 0.024) \cdot 10^{-10}$ m, four nearest protons of NH_4^+ - cation are displaced at the distance $r_{\text{N-H}} = (1.038 \pm 0.04) \cdot 10^{-10}$ m from a nitrogen nucleus, and the neighboring protons are spaced from each other to the distance $r_{\text{H-H}} = (1.695 \pm 0.04) \cdot 10^{-10}$ m [22].

Below 242.9 K, the crystal is in its ordered phase. The equilibrium disposition of atoms is shown in Figure 1. The random local motion of ammonium ions does not change the ordered structure of the crystal. It means that the reorientation symmetry group of any ammonium ion vector is the point symmetry group of tetrahedron T.

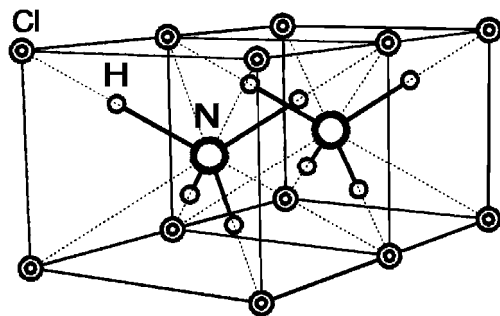


Figure 1: Schematic of the NH_4Cl crystal structure in the ordered phase ($T < 242.9$ K).

In the single crystal of NH_4Cl , Bersohn and Gutowsky have investigated the proton resonance spectra [18] and we have measured the proton spin-lattice relaxation times [10]. It was found that both the shape of spectral line and the relaxation times are anisotropic and show temperature dependence. To discuss the continuous wave data the quantum mechanical calculation were applied, but no extra knowledge was added about crystal structure [18]. The proton relaxation data were discussed in the framework of classical mechanical EAJM-approach taken as the model of NH_4^+ cation HMM [2, 8]. As a result of such simulation, a phenomenon of the site symmetry distortion was discovered in the ordered phase of NH_4Cl .

In the following description, we shall simulate particular contributions to the proton NMR 2nd moment in the single crystal of NH_4Cl for slow and fast motion regimes of NH_4^+ cation (low and high temperature regions) by using Equations (15), (16), (20), and (21), first. Then, we shall approximate the experimental curves of temperature dependence ($-200^\circ\text{C} < T < 25^\circ\text{C}$) of the total 2nd moment M_2 [18] by general Equation (22) for two orientations of the NH_4Cl single crystal in the static magnetic field: $[1,0,0] \parallel \mathbf{B}_0$ and $[1,1,0] \parallel \mathbf{B}_0$.

We shall calculate the particular contributions to the angular dependent second moment of proton NMR spectral line stimulated by

- interaction between the inner four proton spins, which gives rise intraionic proton-proton contribution – $M_{2,\text{HH}}^{(\text{intra})}$
- action of the unique inner nitrogen nuclear spin to 4 proton spins, which produces the intraionic nitrogen-proton contribution – $M_{2,\text{NH}}^{(\text{intra})}$
- action of 104 nearest adjacent proton spins to 4 proton spins of target NH_4^+ cation giving rise the interionic proton-proton contribution – $M_{2,\text{HH}}^{(\text{inter})}$
- action of 8 nearest adjacent chlorine spins to 4 proton spins of the target NH_4^+ cation giving rise the interionic chlorine-proton contribution $M_{2,\text{ClH}}^{(\text{inter})}$, and
- action of 6 nearest adjacent nitrogen spins to 4 proton spins of the target NH_4^+ cation giving rise the interionic nitrogen-proton contribution – $M_{2,\text{NH}}^{(\text{inter})}$

All actions of other nuclear spins to the target proton spins are neglected here. Due to their remoteness, they give a small effect in the studied 2nd moment.

- Slow motion regime of NH_4^+ cation
 - Intraionic proton-proton contribution – $M_{2,\text{HH}}^{(\text{intra})}(\phi, \vartheta)$

Accounting for the values of proton spin $I_j = I_{\text{H}} = 1/2$ and the number of protons $N_i = N_{\text{H}} = 4$ in Equation (15), we shall get the rated expression of $M_{2,\text{HH}}^{(\text{intra})}(\phi, \vartheta)$ by:

$$M_{2,\text{HH}}^{(\text{intra})}(\phi, \vartheta) = \frac{27}{4} \gamma_{\text{H}}^2 \hbar^2 r_{\text{HH}}^{-6} \sum_{\alpha=1,2} \left(\sum_{l=0}^2 q_{\alpha} a_{\alpha l 0}(\phi) \cos^{2l} \vartheta \right). \quad (23)$$

Substituting in Equation (23) 1) table data: $\gamma_H = 26753 \text{ s}^{-1}\text{Gs}^{-1}$ and $\hbar = 1.0544 \cdot 10^{-27} \text{ erg}\cdot\text{s}$; 2) experimental values: $q_1 = 0.25$, $q_2 = 0.73$ [10, 11], $r_{\text{HH}} = 1.695 \cdot 10^{-8} \text{ cm}$ [22], and 3) expressions of the factors $a_{\omega 0}(\phi)$ [2, 8]: $a_{100}(\phi) = (1/8)(1+3\cos^2 2\phi)$, $a_{110}(\phi) = -(3/4)(1+\cos^2 2\phi)$, $a_{120}(\phi) = (3/8)(3+\cos^2 2\phi)$, $a_{200}(\phi) = (1/4)(1-\cos^2 2\phi)$, $a_{210}(\phi) = (1/2)(1+\cos^2 2\phi)$, and $a_{200}(\phi) = -(1/4)(3+\cos^2 2\phi)$ allows us to obtain the explicit expression of $M_{2,\text{HH}}^{(\text{intra})}(\phi, \vartheta)$ by

$$M_{2,\text{HH}}^{(\text{intra})}(\phi, \vartheta) = 48.39 - 20.09[\cos^2 2\phi + 2(1+\cos^2 2\phi)\cos^2 \vartheta - (3+\cos^2 2\phi)\cos^4 \vartheta]. \quad (24)$$

The surface-plot graph of $M_{2,\text{HH}}^{(\text{intra})}(\phi, \vartheta)$, the HH-intraionic part of the proton NMR 2nd moment, drawn according to Equation (24) as a function of spherical angles ϕ and ϑ of the crystal orientation in the static magnetic field for a slow motion regime of NH_4^+ cation in NH_4Cl single crystal is presented in Figure 2a. The graph of $M_{2,\text{HH}}^{(\text{intra})}(\vartheta)$, abridged dependence $M_{2,\text{HH}}^{(\text{intra})}$ of the polar angle ϑ , while the azimuthal angle ϕ is fixed by $\pi/4$, is shown in Figure 2b.

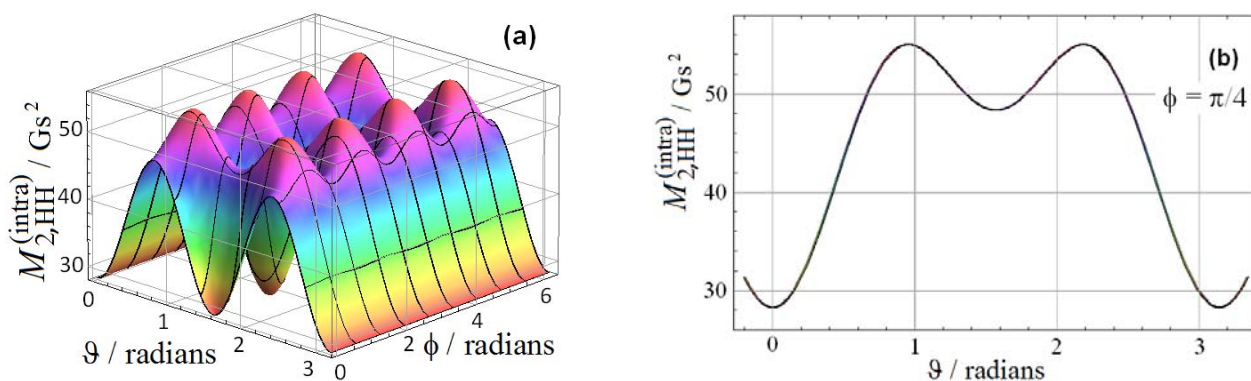


Figure 2: The graphs of the theoretical angular dependence of HH-intraionic contribution $M_{2,\text{HH}}^{(\text{intra})}$ to the proton NMR 2nd moment in NH_4Cl single crystal drawn for a slow motion regime of NH_4^+ cation according to Equation (24) as a function: a) of spherical angles ϕ and ϑ , b) of polar angle ϑ for $\phi = \pi/4$.

ii. Intraionic nitrogen-proton contribution – $M_{2,\text{NH}}^{(\text{intra})}(\phi, \vartheta)$

By substituting the number of protons $N_i = 4$, the number of nitrogen spins $N_s = 1$, Plank constant $\hbar = 1.054 \cdot 10^{-27} \text{ erg}\cdot\text{s}$, the nitrogen spin value $I_s = I_N = 1$ and gyromagnetic ratio $\gamma_N = 1933.3 \text{ s}^{-1}\text{Gs}^{-1}$, and experimental values of dynamic weights: $q_1 = 0.25$, $q_2 = 0.73$ [10, 11], $r_{\text{NH}} = 1.038 \cdot 10^{-8} \text{ cm}$ [22], and expressions of the factors $a_{\omega 0}(\phi)$: $a_{100}(\phi) = (1/8)(1+3\cos^2 2\phi)$, $a_{110}(\phi) = -(3/4)(1+\cos^2 2\phi)$, $a_{120}(\phi) = (3/8)(3+\cos^2 2\phi)$, $a_{200}(\phi) = (1/4)(1-\cos^2 2\phi)$, $a_{210}(\phi) = (1/2)(1+\cos^2 2\phi)$, and $a_{200}(\phi) = (1/4)(3+\cos^2 2\phi)$ [2, 8] in Equation (16), we are obtaining the expression of $M_{2,\text{NH}}^{(\text{intra})}(\phi, \vartheta)$ in the explicit form by

$$M_{2,\text{NH}}^{(\text{intra})}(\phi, \vartheta) = 0.786263 [\cos^2 2\phi + 2(1+\cos^2 2\phi)\cos^2 \vartheta - (3+\cos^2 2\phi)\cos^4 \vartheta]. \quad (25)$$

The surface-plot graph $M_{2,\text{NH}}^{(\text{intra})}(\phi, \vartheta)$, the intraionic NH-contribution to the proton NMR 2nd moment, drawn according to Equation (25) as a function of spherical angles ϕ and ϑ of the crystal orientation in the static magnetic field for a slow motion regime of NH_4^+ cation in NH_4Cl single crystal is presented in Figure 3a. The plane graph $M_{2,\text{NH}}^{(\text{intra})}(\vartheta)$ drawn according to Equation (25) as a function of solely polar angle ϑ is presented in Figure 3b, whereas azimuth angle is fixed by $\phi = \pi/4$.

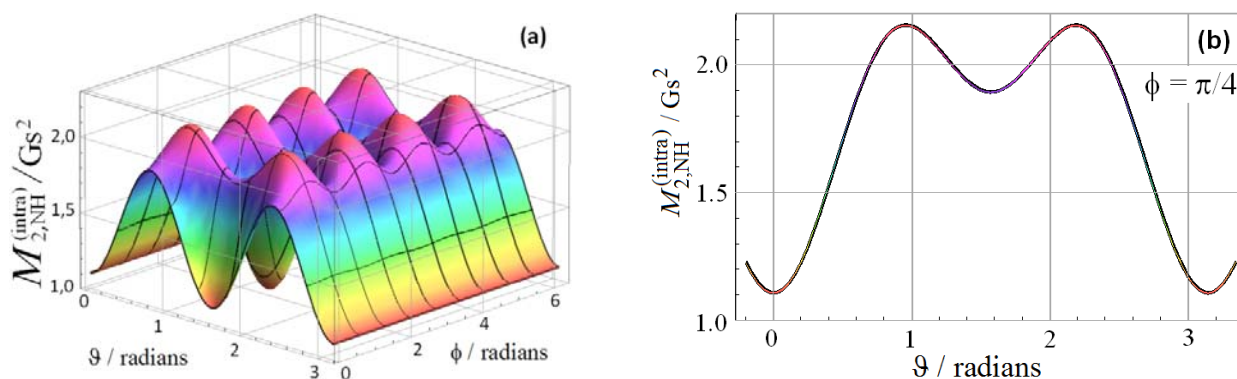


Figure 3: The graphs $M_{2,NH}^{(intra)}(\phi, \vartheta)$ and $M_{2,NH}^{(intra)}(\vartheta)$ of NH-intraionic contribution to the proton NMR second moment in NH_4Cl single crystal drawn according to Equation (25) for a slow motion regime of NH_4^+ -cation as functions of: a) spherical angles ϕ and ϑ and b) polar angle ϑ for $\phi = \pi/4$, respectively.

iii. Interionic proton-proton contribution – $M_{2,HH}^{(inter)}(\phi, \vartheta)$

The schematic of target NH_4^+ -ion with inner protons numerated by 1, 2, 3, and 4 is shown in Figure 4. Besides, 26 neighboring NH_4^+ -ions are presented therein. During this simulation, we shall assume that all protons are immobile and confine ourselves to 104 nearest outer protons, from which only four protons numerated by 5, 6, 7, and 8 are shown in Figure 4. Now, we shall write an expression describing interionic HH-contribution of only 104 nearest protons to inner 4 protons $M_{2,HH}^{(inter)}(\phi, \vartheta)$:

$$M_{2ji}^{(inter)}(\phi, \vartheta) = \frac{48\pi^2}{25N_i} \sum_{i=1}^{N_i} \sum_{j'=5}^{108} \hbar^2 \gamma_i^2 r_{ji}^{-6} I_i(I_i + 1) \left[\sum_{m=-2}^2 Y_m^{(2)}(\phi, \vartheta) Y_m^{(2)}(\varphi_{j'i}, \theta_{j'i}) \right]^2, \quad (26)$$

where for commodity the outer protons are labeled by j' ($5 \leq j' \leq 108$). By substituting the numbering values of constants γ_{HH} and \hbar , just presented, $I_i = I_H = 1/2$, $N_i = 4$, Equation (26) takes the following semi explicit form:

$$M_{2,HH}^{(inter)}(\phi, \vartheta) = 2.82721 \cdot 10^{-45} \sum_{j'=5}^{108} \sum_{i=1}^4 \left| \sum_{m=-2}^2 Y_m^{(2)}(\phi, \vartheta) Y_m^{(2)}(\varphi_{j'i}, \theta_{j'i}) \right|^2 r_{ji}^{-6}, \quad (27)$$

where the values of proton-proton distances r_{ji} and angles $\varphi_{j'i}$ and $\theta_{j'i}$ are to be estimated by using the structure data [22]: $r_{ClCl} = r_{NN} = 3.844 \cdot 10^{-10}$ m, $r_{NH} = 1.038 \cdot 10^{-10}$ m, $r_{HH} = 1.695 \cdot 10^{-10}$ m.

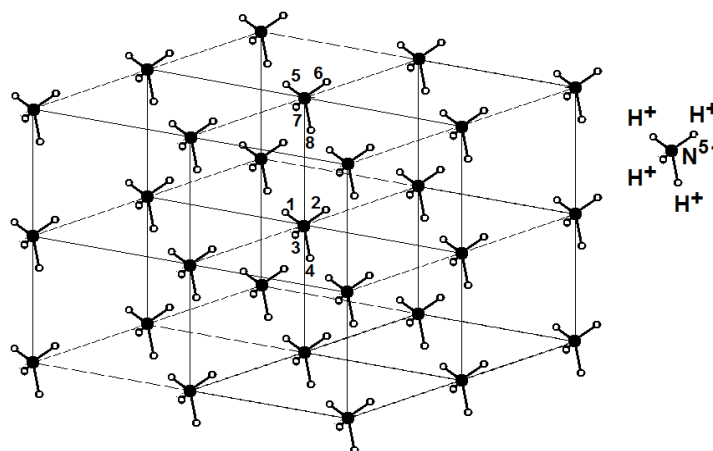


Figure 4: The disposition of hydrogen and nitrogen nuclei in NH_4Cl single crystal taken into account by evaluating the interionic contributions to the 2nd moment of proton NMR spectral line. The numbers counted from 1 to 4 numerates the target protons and the numbers from 5 to 8 label the protons of an adjacent arbitrary chosen NH_4^+ -cation. The chlorine ions are not displayed in Figure 4. They are presented in Figure 1

The surface plot graph of $M_{2,HH}^{(inter)}(\phi, \vartheta)$, the HH-interionic contribution to the proton NMR 2nd moment of ammonium chloride single crystal drawn according to Equation (27) as a function of spherical angles ϕ and ϑ of the crystal orientation in the static magnetic field for a slow motion regime of NH_4^+ -cations is shown in Figure 5a. The plan graph of $M_{2,HH}^{(inter)}(\vartheta)$, the graph $M_{2,HH}^{(inter)}(\phi, \vartheta)$ for $\phi = \pi/4$, is shown in Figure 5b.

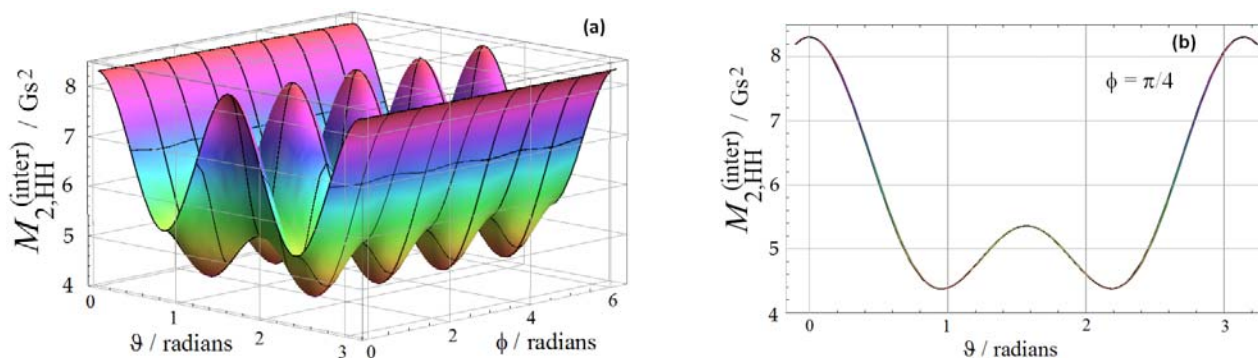


Figure 5: The graphs of $M_{2,HH}^{(inter)}(\phi, \vartheta)$ and $M_{2,HH}^{(inter)}(\vartheta)$, the HH-interionic contribution to the proton NMR 2nd moment in ammonium chloride single crystal, drawn according to Equation (27) as functions of spherical angles ϕ and ϑ (Figure 5a) and polar angle ϑ for $\phi = \pi/4$ (Figure 5b) of the crystal orientation in the static magnetic field for a slow motion regime of NH_4^+ -cations.

iv. *Interionic nitrogen-proton contribution – $M_{2,NH}^{(inter)}(\phi, \vartheta)$*

By substituting constant values $\hbar = 1.0544 \cdot 10^{-27}$ erg.s, $\gamma_v = \gamma_N = 1933.3 \text{ s}^{-1}\text{Gs}^{-1}$, $I_v = I_N = 1$, the numbers of protons $N_i = 4$ and nitrogen nuclei $N_v = N_N = 6$ in Equation (21), we are getting the rated expression of interionic contribution created by 6 nearest nitrogen nuclear spins for a slow motion regime of NH_4^+ -cations:

$$M_{2,NH}^{(inter)}(\phi, \vartheta) = 1.75 \cdot 10^{-47} \sum_{v=1}^6 \sum_{i=1}^4 \left| \sum_{n=-2}^2 Y_n^{(2)}(\phi, \vartheta) Y_n^{(2)}(\varphi_{vi}, \theta_{vi}) \right|^2 r_{vi}^{-6}. \quad (28)$$

The graphs of $M_{2,NH}^{(inter)}(\phi, \vartheta)$ and $M_{2,NH}^{(inter)}(\vartheta)$ similar to those of $M_{2,HH}^{(inter)}(\phi, \vartheta)$ and $M_{2,HH}^{(inter)}(\vartheta)$ displayed in Figure 5 are shown in Figure 6:

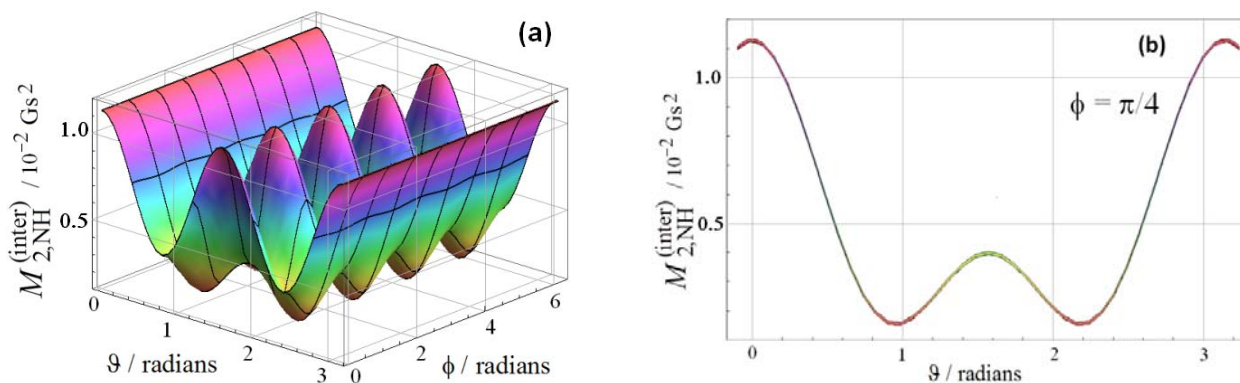


Figure 6: The graphs of $M_{2,NH}^{(inter)}(\phi, \vartheta)$ and $M_{2,NH}^{(inter)}(\vartheta)$, the interionic NH-contribution to the proton NMR 2nd moment in ammonium chloride single crystal drawn according to Equation (28) as functions of spherical angles ϕ and ϑ (Figure 6a) and ϑ for $\phi = \pi/4$ (Figure 6b) of the crystal orientation in the static magnetic field for a slow motion regime of NH_4^+ -cations.

v. *Interionic chlorine-proton contribution – $M_{2,ClH}^{(inter)}(\phi, \vartheta)$*

By substituting constant values $\hbar = 1.0544 \cdot 10^{-27}$ erg.s, $\gamma_v = \gamma_{Cl} = 2557.3 \text{ s}^{-1}\text{Gs}^{-1}$, $I_v = I_{Cl} = 3/2$, the number of protons $N_i = N_H = 4$ and the number of chlorine spins $N_v = N_{Cl} = 8$, the rated expression of the heteronuclear interionic ClH-contribution $M_{2,ClH}^{(inter)}(\phi, \vartheta)$ follows from Equation (21):

$$M_{2,\text{ClH}}^{(\text{inter})}(\phi, \vartheta) = 5.42 \cdot 10^{-47} \sum_{v=1}^8 \sum_{i=1}^4 \left| \sum_{n=-2}^2 Y_n^{(2)}(\phi, \vartheta) Y_n^{(2)}(\varphi_{vi}, \theta_{vi}) \right|^2 r_{vi}^{-6}. \quad (29)$$

The graphs of $M_{2,\text{ClH}}^{(\text{inter})}(\phi, \vartheta)$ and $M_{2,\text{ClH}}^{(\text{inter})}(\vartheta)$, similar to those of $M_{2,\text{HH}}^{(\text{inter})}(\phi, \vartheta)$ and $M_{2,\text{HH}}^{(\text{inter})}(\vartheta)$ presented in Figure 5, are shown in Figure 7.

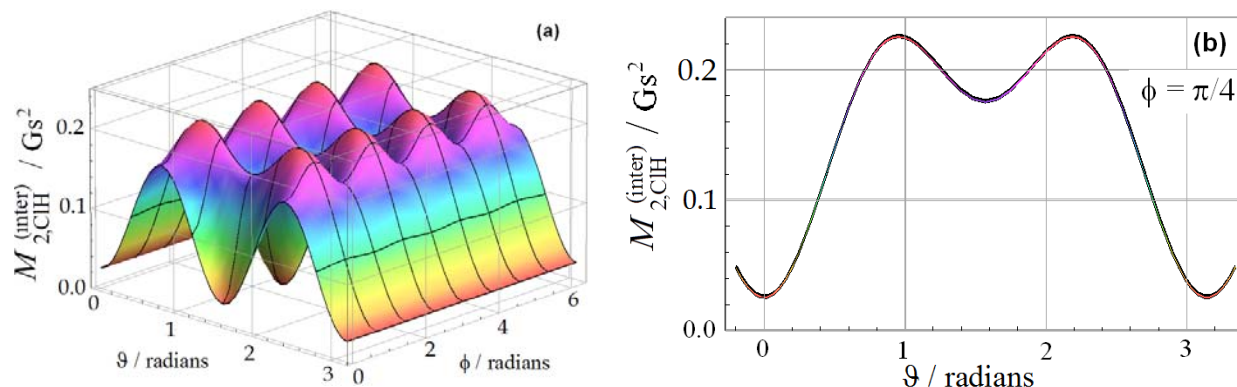


Figure 7: The graphs of $M_{2,\text{ClH}}^{(\text{inter})}(\phi, \vartheta)$ and $M_{2,\text{ClH}}^{(\text{inter})}(\vartheta)$, the interionic ClH-contribution to the proton NMR 2nd moment in ammonium chloride single crystal, drawn according to Equation (29) as functions of a) spherical angles ϕ and ϑ and b) polar angle ϑ ($\phi = \pi/4$) of the crystal orientation in the static magnetic field for a slow motion regime of NH_4^+ -cations.

vi. Total proton 2nd moment for the slow motion regime of NH_4^+ -cation – $M(\phi, \vartheta)$

Summing the partial contributions to M_2 given by Equations (24), (25), (27), (28), and (29), we are getting the expression of the total proton 2nd moment $M_2(\phi, \vartheta)$ in the semiexplicit form as a function of polar ϑ and azimuthal ϕ angles of the NH_4Cl crystal orientation in the static magnetic field for the slow motion regime of NH_4^+ -cation:

$$\begin{aligned} M_2(\phi, \vartheta) = & 50.28 - 20.88 \cdot \cos^2 2\phi + 41.76 \cdot (1 + \cos^2 2\phi) \cdot \cos^2 \vartheta - 20.88 \cdot (3 + \cos^2 2\phi) \cdot \cos^4 \vartheta \\ & + 2.83 \cdot 10^{-45} \cdot \sum_{i=1}^4 \sum_{j'=5}^{108} \left| \sum_{m=-2}^2 Y_m^{(2)}(\phi, \vartheta) Y_m^{(2)}(\varphi_{vi}, \theta_{vi}) \right|^2 r_{j'i}^{-6} + \\ & 1.75 \cdot 10^{-47} \sum_{v=1}^6 \sum_{i=1}^4 \left| \sum_{n=-2}^2 Y_n^{(2)}(\phi, \vartheta) Y_n^{(2)}(\varphi_{vi}, \theta_{vi}) \right|^2 r_{vi}^{-6} \\ & 5.42 \cdot 10^{-47} \sum_{v=1}^8 \sum_{i=1}^4 \left| \sum_{n=-2}^2 Y_n^{(2)}(\phi, \vartheta) Y_n^{(2)}(\varphi_{vi}, \theta_{vi}) \right|^2 r_{vi}^{-6} +, \end{aligned} \quad (30)$$

where the distances $r_{j'i}$ and r_{vi} are indicated in cm ($1\text{cm} = 10^{-2}\text{ m}$) and the 2nd moment – in Gs^2 ($1\text{Gs} = 10^{-4}\text{ T}$). The spherical harmonics $Y_n^{(2)}(\phi, \vartheta)$, $Y_m^{(2)}(\varphi_{vi}, \theta_{vi})$ and $Y_m^{(2)}(\varphi_{vi}, \theta_{vi})$ are defined as built-in functions of the software Wolfram Mathematica™. The graph of the theoretical angular dependence of the total proton 2nd moment $M_2(\phi, \vartheta)$ drawn by Equation (30) are presented in Figure 8a.

In Figure 8b, the graph of the theoretical dependence of the total proton 2nd moment is shown as a function of polar angle ϑ for the azimuthal angle fixed by $\phi = \pi/4$. At that orientation of the crystal, the values of the 2nd moment can be determined along all principal axes of the cubic unit cell. The experimental values of the second moment at low temperature (-195°C), that is in the ordered phase, has been found equal to $36.5\text{ Gs}^2 \pm 0.7\text{ Gs}^2$ for the direction of static magnetic field vector oriented alongside the fourfold symmetry axis $\mathbf{B}_0 \parallel [1,0,0]$, and $54.6\text{ Gs}^2 \pm 0.6\text{ Gs}^2$ – alongside the twofold symmetry axis $\mathbf{B}_0 \parallel [1,1,0]$ [18]. These values calculated by using our theoretical formula given by Equation (30) are equal to $37.75\text{ Gs}^2 \pm 1.5\text{ Gs}^2$ and $55.82\text{ Gs}^2 \pm 2.5\text{ Gs}^2$, respectively, which agree satisfactorily with those experimentally determined.

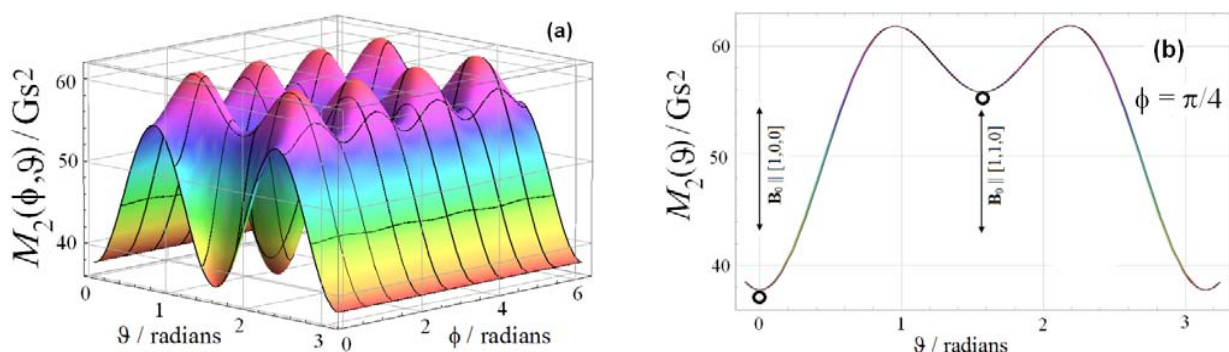


Figure 8: The graphs of the theoretical angular dependence of the proton NMR total 2nd moment in ammonium chloride single crystal for a slow motion regime of NH₄⁺ cation:

a) $M_2(\phi, \theta)$ and b) $M_2(\theta)$. The graph of $M_2(\theta)$ is drawn for $\phi = \pi/4$. Experimental values of $M_2(\theta)$ mapped by open circles are given for two directions of the static magnetic field in the unit cell of NH₄Cl [18]: $\mathbf{B}_0 || [1,0,0]$ and $\mathbf{B}_0 || [1,1,0]$.

c) *Fast motion regime of NH₄⁺ -cation*

i. *Overview*

Fast motion of ammoniums taking place at high temperatures follows decreasing the intraionic contributions down to zero: $M_{2,HH}^{(intra)}(\phi, \theta) = 0$ and $M_{2,NH}^{(intra)}(\phi, \theta) = 0$, whereas interionic ones decrease partially. Therefore, the residual proton 2nd moment in the fast motion regime of NH₄Cl reduces down to 3 additive residual interionic contributions: $M_{2,HH}^{(inter-res)}(\phi, \theta)$, $M_{2,NH}^{(inter-res)}(\phi, \theta)$, and $M_{2,ClH}^{(inter-res)}(\phi, \theta)$.

Hindered rotation of ammoniums averages the internuclear vectors of relevant dipole-dipole interactions. Hence, in order to compute the terms $M_{2,HH}^{(inter-res)}(\phi, \theta)$, $M_{2,NH}^{(inter-res)}(\phi, \theta)$ and $M_{2,ClH}^{(inter-res)}(\phi, \theta)$ in the fast motion regime of NH₄⁺-cations, the spin-spin distances have to be replaced by those dynamically averaged, in the formulae (27), (28), and (29). We shall assume that the average proton-proton distances $\langle r_{HH} \rangle$ between the protons of adjacent NH₄⁺-cations in the first coordinate sphere will be taken equal to the lattice parameter $\langle r_{HH} \rangle_1 = r_{NN} = 3.844 \cdot 10^{-8}$ cm. Relative distances in the second and third coordinate spheres will respectively equal to $\langle r_{HH} \rangle_2 = \sqrt{2} \cdot r_{NN}$ and $\langle r_{HH} \rangle_3 = \sqrt{3} \cdot r_{NN}$. In agreement with crystal structure, the distances $r_{vi} = \langle r_{NH} \rangle$ and $r_{vi} = \langle r_{ClH} \rangle$ cited in Equations (28) and (29) have to be replaced by relative average values $\langle r_{NH} \rangle = r_{NN}$ and $\langle r_{ClH} \rangle = \sqrt{3}/2 \cdot r_{NN}$.

The three- and two-dimensional theoretical graphs of the partial interionic 2nd moment $M_{2,HH}^{(inter-res)}(\phi, \theta)$, $M_{2,NH}^{(inter-res)}(\phi, \theta)$, and $M_{2,ClH}^{(inter-res)}(\phi, \theta)$ are presented for the NH₄⁺-cation fast motion regime as functions of polar angle θ and azimuth angle ϕ in Figures 9-11 (a) and as a function of polar angle θ , whereas the azimuth angle ϕ is fixed by $\phi = \pi/4$, in Figures 9-11 (b). The graphs of Figures 12 display the total 2nd moment in the fast motion regime.

ii. *Interionic proton-proton contribution – $M_{2,HH}^{(inter-res)}(\phi, \theta)$*

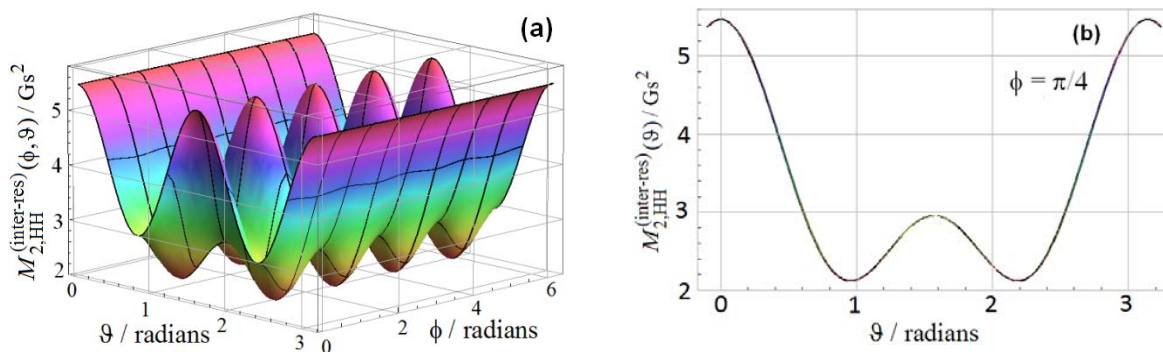


Figure 9: The graphs of $M_{2,HH}^{(inter-res)}(\phi, \theta)$ and $M_{2,HH}^{(inter-res)}(\theta)$, the HH-interionic contribution to the proton NMR 2nd moment in ammonium chloride single crystal, drawn according to Equation (27) as functions of spherical angles ϕ and θ (Figure 9a) and polar angle θ for $\phi = \pi/4$ (Figure 9b) of the crystal orientation in the static magnetic field for a fast motion regime of NH₄⁺-cations. The HH-distances were taken as average values by $\langle r_{HH} \rangle_1 = r_{NN}$, $\langle r_{HH} \rangle_2 = \sqrt{2} \cdot r_{NN}$, and $\langle r_{HH} \rangle_3 = \sqrt{3} \cdot r_{NN}$ ($r_{NN} = 3.844 \cdot 10^{-8}$ cm).

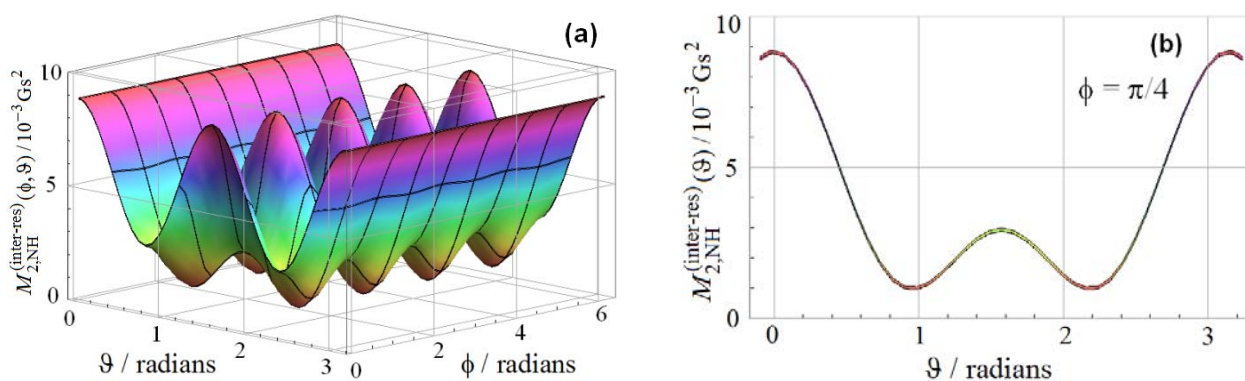
iii. Interionic nitrogen-proton contribution – $M_{2,\text{NH}}^{(\text{inter-res})}(\phi, \vartheta)$


Figure 10: The graphs of $M_{2,\text{NH}}^{(\text{inter-res})}(\phi, \vartheta)$ and $M_{2,\text{NH}}^{(\text{inter-res})}(\vartheta)$, the NH-interionic contribution to the proton NMR 2nd moment in ammonium chloride single crystal, drawn according to Equation (28) as functions of spherical angles ϕ and ϑ (Figure 10a) and polar angle ϑ for $\phi = \pi/4$ (Figure 10b) of the crystal orientation in the static magnetic field for a fast motion regime of NH_4^+ -cations. The NH-distances were taken as average values by $\langle r_{\text{NH}} \rangle = r_{\text{NN}}$ ($r_{\text{NN}} = 3.844 \cdot 10^{-8}$ cm).

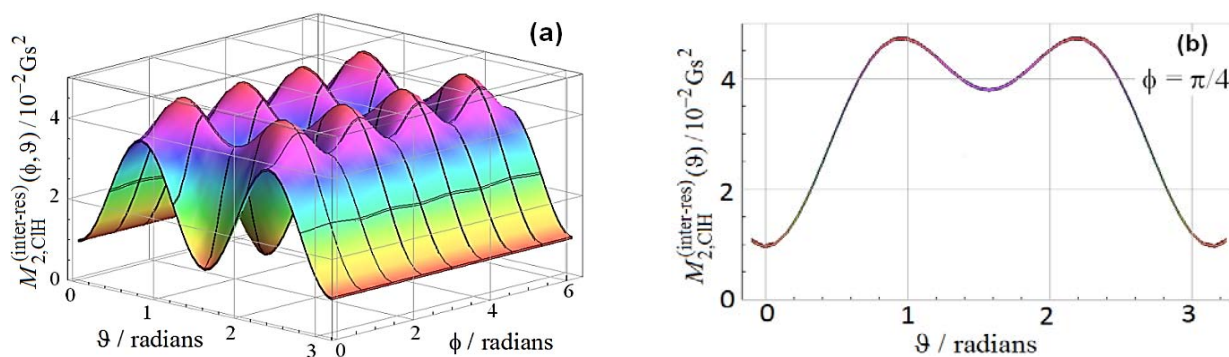
 iv. Interionic chlorine-proton contribution – $M_{2,\text{ClH}}^{(\text{inter-res})}(\phi, \vartheta)$


Figure 11: The graphs of $M_{2,\text{ClH}}^{(\text{inter-res})}(\phi, \vartheta)$ and $M_{2,\text{ClH}}^{(\text{inter-res})}(\vartheta)$, the ClH-interionic contribution to the proton NMR 2nd moment in ammonium chloride single crystal, drawn according to Equation (29) as functions of spherical angles ϕ and ϑ (Figure 11a) and polar angle ϑ for $\phi = \pi/4$ (Figure 11b) of the crystal orientation in the static magnetic field for a fast motion regime of NH_4^+ -cations. The ClH-distances were taken as average values by $\langle r_{\text{ClH}} \rangle = 3/2 \cdot r_{\text{NN}}$ ($r_{\text{NN}} = 3.844 \cdot 10^{-8}$ cm).

v. Total proton 2nd moment for the fast motion regime of NH_4^+ -cation – $M_2^{(\text{res})}(\phi, \vartheta)$

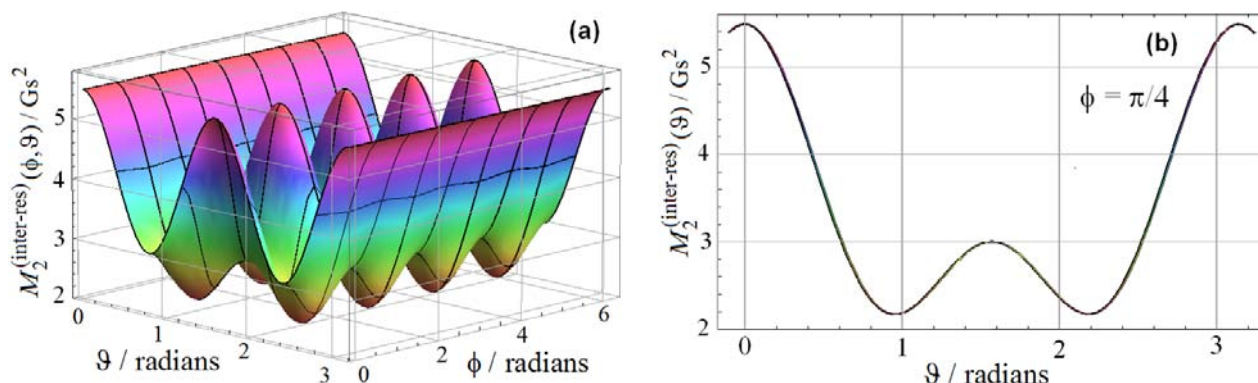


Figure 12: The graphs of $M_2^{(\text{inter-res})}(\phi, \vartheta)$ and $M_2^{(\text{inter-res})}(\vartheta)$, the total residual proton NMR 2nd moment in ammonium chloride single crystal, drawn according to Equation (30) as functions of spherical angles ϕ and ϑ (Figure 12a) and polar angle ϑ for $\phi = \pi/4$ (Figure 12b) of the crystal orientation in the static magnetic field for a fast motion regime of NH_4^+ -cations.

vi. Temperature dependence of the total proton 2nd moment $M_2(\phi, \vartheta)$ for 2 selected directions in NH_4Cl

To describe $M_2^{(T)}(0, 0)$ and $M_2^{(T)}(\pi/4, \pi/2)$, the experimental temperature dependences of the total proton NMR 2nd moment for 2 directions of NH_4Cl in the external magnetic field: $[1, 0, 0] \uparrow \uparrow \mathbf{B}_0$ (e.g. $\phi = 0, \vartheta = 0$) and $[1, 1, 0] \uparrow \uparrow \mathbf{B}_0$ (e.g. $\phi = \pi/4, \vartheta = \pi/2$) [21], we shall use Equations (9)-(10) reduced to $\tau_a = \tau = \tau_0 \exp(E_a/RT)$ and Equations (24, 25, 27-29). Performing necessary calculations, we are obtaining the rated expression of $M_2^{(T)}(0, 0)$ by

$$M_2^{(T)}(0, 0) = 5.50 + 32.25 \cdot \frac{2}{\pi} \cdot \arctg[4257 \cdot \delta B_H(0, 0) \cdot \tau_0 \cdot \exp\left(\frac{E_a}{RT}\right)] \quad (31)$$

and the rated expression of $M_2^{(T)}(\pi/4, \pi/2)$ by

$$M_2^{(T)}(\pi/4, \pi/2) = 3.00 + 52.8 \cdot \frac{2}{\pi} \cdot \arctg[4257 \cdot \delta B_H(\pi/4, \pi/2) \cdot \tau_0 \cdot \exp\left(\frac{E_a}{RT}\right)]. \quad (32)$$

Here, $\delta B_H(0, 0)$ and $\delta B_H(\pi/4, \pi/2)$ are the proton NMR line widths expressed in Gauss for directions $[1, 0, 0] \uparrow \uparrow \mathbf{B}_0$ and $[1, 1, 0] \uparrow \uparrow \mathbf{B}_0$ in the slow motion regime, τ_0 is the time interval between two successive attempts to overlap the reorientation barrier, and E_a is the HMM activation energy. By using Equations (31) and (32) and the constant values $\delta B_H(0, 0) = 19.5$ Gs, $\delta B_H(\pi/4, \pi/2) = 23.3$ Gs [21] and $E_a = 4.83$ kcal/mol [2], we approximated the proton NMR experimental data of $M_2[1, 0, 0]$ and $M_2[1, 1, 0]$ with the help of computer program "Origin Lab-Origin 2016™". The corresponding graphical results are shown in Figure 13. The present approximation allowed us to determine the time constant τ_0 to be equal to $6.09 \cdot 10^{-14}$ s and $5.01 \cdot 10^{-14}$ s for crystal orientations $[1, 0, 0] \uparrow \uparrow \mathbf{B}_0$ and $[1, 1, 0] \uparrow \uparrow \mathbf{B}_0$, respectively. From relaxation measurements performed in rotating reference frame, the corresponding values of τ_0 were extrapolated to $8.4 \cdot 10^{-14}$ s and $9.4 \cdot 10^{-14}$ s [2]. For the reason that the quantity τ_0 has a meaning of adjustable parameters in NMR-spectroscopy, we are concluding that the agreement found under the order of greatness amongst the experimental data of τ_0 is satisfactorily.

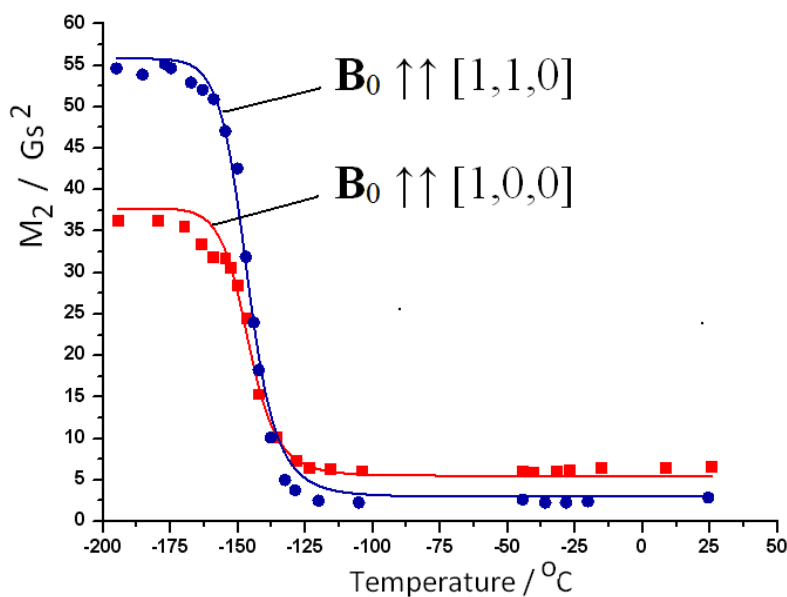


Figure 13: Temperature dependence of the 2nd moment of proton NMR absorption spectral line in the single crystal of ammonium chloride. Experimental data mapped for direction $[1,0,0]\uparrow\uparrow B_0$ are shown by square symbols “■” and for direction $[1,1,0]\uparrow\uparrow B_0$ – by round symbols “●” [21]. Theoretical lines are drawn by using Equations (31) and (32), constant values $\delta B_H(0,0) = 19.5$ Gs ($[1,0,0]\uparrow\uparrow B_0$) and $\delta B_H(\pi/4,\pi/2) = 23.3$ Gs ($[1,1,0]\uparrow\uparrow B_0$) [21] and $E_a = 4.83$ kcal/mol [2].

IV. DISCUSSION

The presented approach to simulating the NMR 2nd moment in molecular crystals, in general, and, particularly, the angular and temperature dependence of the proton NMR 2nd moment in ammonium chloride allowed us to take new quantitative knowledge on the structure and molecular dynamics herein. In the Table, the theoretical values of different contributions to the 2nd moment are exposed for main orientations of the NH_4Cl crystal at slow and fast hindered motion regimes. NH_4^+ -cation slow motion regime is observed at low temperatures, lower 175°C (98 K), and dominant contribution to M_2 is $M_{2,HH}^{(intra)}$, which is due to intraionic proton-proton interaction. At high temperatures, higher 100°C (173 K), NH_4^+ -cation fast motion regime is observed and major contribution to M_2 is also defined by proton-proton interaction, but, this time, it is due to interionic one, $M_{2,HH}^{(inter)}$.

Table 1: The theoretical values of the 2nd moment contributions to the proton magnetic resonance spectral line in the single crystal of NH_4Cl at different orientation and motion regimes of NH_4^+ -cation

ORIENTATION	$B_0 \uparrow\uparrow [100]$	$B_0 \uparrow\uparrow [111]$	$B_0 \uparrow\uparrow [110]$
Slow motion regime ($\omega_0\tau_\alpha \gg 0$)			
$M_{2,HH}^{(intra)}, Gs^2$	28.30	55.09	48.39
$M_{2,NH}^{(intra)}, Gs^2$	1.11	2.16	1.89
$M_{2,HH}^{(inter)}, Gs^2$	8.31	4.38	5.35
$M_{2,CH}^{(inter)}, 10^{-2} Gs^2$	2.56	22.66	17.56
$M_{2,NH}^{(inter)}, 10^{-2} Gs^2$	1.13	0.16	0.40
Fast motion regime ($\omega_0\tau_\alpha \ll 0$)			
$M_{2,HH}^{(inter)}, Gs^2$	5.47	2.12	2.96
$M_{2,CH}^{(inter)}, 10^{-2} Gs^2$	0.97	4.73	3.79
$M_{2,NH}^{(inter)}, 10^{-2} Gs^2$	0.88	0.10	0.29

V. CONCLUSIONS

NMR investigation of structure and motion in single-crystals is one of the most powerful analytical methods. While simple approach for understanding of non-standard structures did not exist, this article describes and demonstrates a technique that can be used to cope with the challenges of crystallography. Together with the relaxation measurements, simulating the second moment of spectral lines allows one to perform an accurate analysis of dynamics and geometry of internal motion as well as crystal structure.

In this article, the analytical expressions describing overall angular dependence of the NMR 2nd moment were derived in a simplest and smart way. The theoretical results are expressed in comprehensible analytical form, easy to use. Application to the model crystal of NH₄Cl allowed us to prove the evidence of the tetragonal distortion of crystal structure that takes place in the ordered phase of ammonium chloride. Analyses of the 2nd moment temperature data for two orientations have shown that all parameters associated with the motion can be obtained. These parameters are in satisfactory agreement with those taken from NMR-relaxation and other spectroscopic studies.

REFERENCES RÉFÉRENCES REFERENCIAS

1. Valiev, K.A., Ivanov, E.N., (1973), *Uspehi Fiz. Nauk*, (Moscow, Nauka), 109, 31.
2. Bashirov F., Gaisin N., (2010), *Crystallography Reviews*, 16, 3
3. Rigny P., (1972), *Physica*, 59, 707.
4. Van Vleck, J.H., (1948), *Phys. Rev.*, 74, 1168.
5. Abragam, A., (1961), *The Principles of Nuclear Magnetism* (Oxf. Univ. Press: N.Y.).
6. Lösche, A., (1962), *Kerninduktion* (Veb Deutscher Verlag der Vissensch.: Berlin)
7. Goc, R.Z., (2002), *Naturforsch.*, 57a, 29.
8. Bashirov, F., (2012), *Spectroscopic Techniques and Hindered Molecular Motion* (CRC Press: London–New York).
9. Bashirov, F.I., (1994), *Extended abstracts of XXVIIth Congress AMPERE, Magnetic Resonance and Related Phenomena*, Kazan: KFTI-Kazan, 1, 282.
10. Bashirov, F.I., (1996) *J. Magn. Res. A* 222, 1.
11. Bashirov, F.I., (1997), *Mol. Phys.*, 91, 281.
12. Bashirov, F.I., (2001), *Crystallography Reports*, 46, 494.
13. Bashirov, F.I., Gaisin, N.K., (1998), *J. Ram. Spectroscopy*, 29, 131.
14. Bashirov, F.I., (1999), *Eur. Phys. J. AP*, 8, 99.
15. Bashirov, F.I., Gaisin, N.K., (2009), *CEJP*, 7, 79.
16. Bashirov, F.I., (2001), *Mol. Phys.*, 99, 25.
17. Bashirov, F., Gaisin, N., (2015), *International Journal of Spectroscopy*, Volume 2015, Article ID 701386, <http://dx.doi.org/10.1155/2015/701386>.
18. Bersohn, R., Gutowsky, H.S., (1954), *J. Chem. Phys.*, 22, 651.
19. Powles, J.G., Gutowsky, H.S., (1955), *J. Chem. Phys.*, 23, 1692.
20. Slichter, Ch.P., (1965), *Principles of Magnetic Resonance* (New York: Harper and Row).
21. Wigner, E., (1931), *Gruppentheorie* (Braunschweig Ed.: Berlin).
22. Gutowsky, H.S., Pake, G.E., Bersohn, R.J., (1954), *Chem. Phys.* 22, 643.



This page is intentionally left blank